BIOCHEMISTRY

 Volume 46, Number 50 December 18, 2007

Accelerated Publications

The Collapse of the Tyrosine Z•−Mn Spin−Spin Interaction above ∼100 K Reveals the Spectrum of Tyrosine Z•. An Application of Rapid-Scan EPR to the Study of Intermediates of the Water Splitting Mechanism of Photosystem II†

Georgia Zahariou, Nikolaos Ioannidis, George Sioros, and Vasili Petrouleas*

Institute of Materials Science, NCSR "Demokritos", 153 10 Aghia Paraskevi Attikis, Greece

Received September 13, 2007; Revised Manuscript Received November 1, 2007

ABSTRACT: Tyr Z of photosystem II mediates electron transfer from the water splitting site, a Mn_4Ca cluster, to the specialized chlorophyll assembly P_{680}. Due to its proton-limited redox properties and the proximity to the Mn cluster, it is thought to play a critical role in the proton-coupled electron transfer reactions that constitute the four-step oxidation mechanism (so-called S-state transitions) of water to molecular oxygen. Spectroscopic evidence for the Tyr Z radical has been scarce in intact preparations (it is difficult to probe it optically, and too short-lived for EPR characterization) until recently. Advances in recent years have allowed the trapping at liquid helium temperatures and EPR characterization of metalloradical intermediates, attributed to tyrosyl Z• magnetically interacting with the Mn cluster. We have extended these studies and examined the evolution of the spectra of five intermediates: $S_0Y_Z^•$, $S_0Y_Z^•$ (with 5% MeOH), $S_1Y_Z^•$, $S_2Y_Z^•$, and $S_2Y_Z^•$ (with 5% MeOH) in the temperature range of 11−230 K. A rapid-scan EPR method has been applied at elevated temperatures. The tyrosyl radical decouples progressively from Mn, as the Mn relaxation rate increases with an increase in temperature. Above ∼100 K, the spectra collapse to the unperturbed spectrum of Tyr Z•, which is found to be somewhat broader than that of the stable Tyr D• radical. This study provides a simple means for recording the spectrum of Tyr Z• and extends earlier observations that link the photochemistry at liquid helium temperatures to the photochemistry at temperatures that support S-state transitions.

Photosystem II is unique among photosystems in that it couples the light-induced charge separation to the splitting of water. A series of four charge separation reactions, initiated by the sequential absorption of four photons by the special chlorophyll assembly P_{680},[1] is required for the oxidation of two water molecules and the evolution of molecular oxygen. The catalytic site of water oxidation, called oxygen evolving complex (OEC), contains a tetranuclear Mn cluster and a Ca^{2+} ion. Transfer of electrons from the OEC to P_{680}^+ is mediated by tyrosine Z, Y_Z. A quinone−iron complex acts as the electron acceptor. The OEC undergoes periodically four one-electron oxidation steps: $S_0 \rightarrow S_1$, ..., $S_3 \rightarrow (S_4)S_0$. Oxygen evolves during the S_3 to (S_4)-S_0 transition, the S_4 being a transient state (*1*−*7*). The oxidizing equivalents during the S-state transitions are stored at or in the immediate vicinity of the Mn cluster. X-ray crystallography has provided in recent years low-resolution images of PSII (*8*−*11*). The least accurate part of the structures is the OEC due to radiation-induced damage of the Mn cluster. With the help of X-ray absorption spectros-

† Financial support of the programs AKMON and ENTEP of the Greek GSRT is kindly acknowledged.

* To whom correspondence should be addressed. Telephone: +301 650-3344. Fax: +301 651-9430. E-mail: vpetr@ims.demokritos.gr.

10.1021/bi7018767 CCC: $37.00
Published on Web 11/17/2007

copy, refined images have been obtained (*12*, *13*), but important aspects of the structure of the OEC are at present unknown. On the other hand, the subtleties of the water oxidizing process can be probed only spectroscopically.

Low-temperature EPR spectroscopy has been applied extensively in the study of individual S states. Less work has been published on intermediates of the S-state transitions involving the Tyr Z$^{\bullet}$ radical in intact (oxygen-evolving) preparations. Tyr Z, due to its proton-limited redox properties (*14*) and the proximity to the Mn cluster (*8*−*11*), is likely to play a critical role (see ref *7* for a recent review of the proposed roles of Tyr Z) in the proton-coupled electron transfer reactions (*15*) during the four-step oxidation mechanism of water to molecular oxygen. Tyr Z$^{\bullet}$ is short-lived in intact samples at ambient temperatures. An earlier study by Hoganson and Babcock (*16*) has demonstrated the great difficulty in recording the spectrum of Tyr Z$^{\bullet}$ at ambient temperatures by a time-resolved technique. These elaborate studies have yielded no more than a noisy spectrum which has been used to confirm that the spectrum of Tyr Z$^{\bullet}$ is not too different from that of Tyr D$^{\bullet}$. Widespread notions in the past excluded formation of this radical by illumination at cryogenic temperatures. The breakthrough observation by Nugent and co-workers (*17*) that samples prepared in the dark-stable S_1 state produced, after visible-light illumination at 11 K, what is now agreeably identified as the $S_1Y_Z^{\bullet}$ intermediate opened the way to the observation of similar intermediates associated with other S states. The work of Nugent et al. (*17*) had actually been preceded by reports (*18*, *19*) of the trapping at liquid-helium temperatures of what was assigned later to $S_2'Y_Z^{\bullet}$ (S_2' indicates a singly deprotonated conformation of S_2) (*20*) and of $S_2''Y_Z^{\bullet}$ (S_2'' in our notation corresponds to a doubly deprotonated S_2 configuration) at alkaline pH (*21*). A number of Tyr Z$^{\bullet}$-based intermediates have been identified and characterized by EPR spectroscopy since, including $S_0Y_Z^{\bullet}$, $S_1Y_Z^{\bullet}$, and $S_2Y_Z^{\bullet}$ and variants of them obtained after treatments that alter the electronic configuration of the OEC but preserve the oxygen evolution [addition of a few percent (v/v) methanol, replacement of Ca^{2+} with Sr^{2+}] (*17*, *22*−*32*; see also ref *27* for a review). These signals are normally produced by direct visible-light illumination at liquid-helium temperatures with the exception of $S_2Y_Z^{\bullet}$ in the absence of methanol, which is trapped by illumination at $\geq$77 K (*28*). Near-IR excitation of the S_2 and S_3 states results in the formation of the $S_1Y_Z^{\bullet}$ and $S_2'Y_Z^{\bullet}$ intermediates, respectively (*19*, *20*, *23*). It has been observed recently that the latter intermediate can also be obtained by visible-light excitation of S_3 (*32*, *33*). The pertinent view is that both intermediates are due to the photochemistry of the Mn cluster itself and not to charge separation (*23*).

A common feature of all the Tyr Z$^{\bullet}$-based intermediates is that the magnetic interaction with the Mn cluster overwhelms the fine and hyperfine features of the tyrosyl radical in the EPR spectra at liquid-helium temperatures. Fielding et al. (*34*) have demonstrated in the past that, in the case of an iron metal center magnetically interacting with a nitroxyl radical species, the electron spin−spin splitting collapses at high temperatures due to the increase in the relaxation rate of the metal as the temperature is increased. As a result, the spectrum obtained at elevated temperatures is that of the unperturbed nitroxyl radical, except with an enhanced relaxation rate. A similar behavior has been demonstrated in the nonfunctional (unable to advance to the S_3 state) S_2 to S_3 intermediate obtained after acetate treatment, attributed to $S_2Y_Z^{\bullet}$ (*35*). While the split EPR signal narrows gradually as the temperature is increased, the observation of a spectrum indistinguishable from that of Tyr D$^{\bullet}$, called signal II, at temperatures above ~100−120 K has been questioned recently by Un et al. (*36*).

Prompted by the experiments of Fielding et al. (*34*) and Szalai et al. (*35*) and the interest to understand the Tyr Z$^{\bullet}$ Mn interaction, and most importantly to examine whether the unperturbed Tyr Z$^{\bullet}$ radical spectrum can be observed in the intact system, we have undertaken a study of the Tyr Z$^{\bullet}$ EPR spectrum as a function of temperature in three different S states. We have examined spectra both in the absence and in the presence of methanol since both −MeOH +MeOH split signals have been reported in the literature. Additionally, the interaction of MeOH with the Mn cluster results in a change in Mn EPR signals from all EPR detectable S states. It also changes all the split signals at low temperatures, and it was interesting to examine whether it has an effect on the tyrosyl radical itself. A rapid-scan EPR method has been applied to record the transient spectra at elevated temperatures. The results show that all metalloradical signals exhibit a behavior similar to that observed first by Fielding et al. (*34*). At elevated temperatures, the spectra collapse to a radical spectrum broader than the spectrum of Tyr D$^{\bullet}$, which is attributed to Tyr Z$^{\bullet}$. This study not only provides a simple means for recording the spectrum of Tyr Z$^{\bullet}$ decoupled from the magnetic interaction with Mn but also extends earlier observations that link the photochemistry at liquid-helium temperatures to the photochemistry at temperatures that support S-state transitions.

MATERIALS AND METHODS

PSII Sample Isolation. PSII-enriched membranes from market spinach (BBY preparations) were isolated by standard procedures (*37*, *38*). Samples for EPR measurements were suspended in a pH 6.5 buffer containing 0.4 M sucrose, 15 mM NaCl, 5 mM $MgCl_2$, and 40 mM MES, at a final chlorophyll concentration of 6−8 mg of chl/mL, and stored in liquid nitrogen. All samples were supplemented with 1 mM duroquinone as an exogenous electron acceptor. No iron oxidation occurs with duroquinone (*39*), and this reduces the number of double hits during flash illumination. Methanol-treated samples were resuspended and washed once in a buffer containing 5% (v/v) methanol, 0.4 M sucrose, 15 mM NaCl, 5 mM $MgCl_2$, and 40 mM MES (pH 6.5) at 6−8 mg of Chl/mL.

[1] Abbreviations: PSII, photosystem II; OEC and WOC, oxygen-evolving complex and water-oxidizing complex, respectively (Mn_4Ca complex also called Mn cluster); S states, S_0−S_4 oxidation states of the OEC; Tyr Z or Y_Z, tyrosine 161 of the D2 protein; Tyr D or Y_D, tyrosine 160 of the D1 protein; P_{680}, primary electron donor in PSII; Signal II, EPR signal of Tyr D$^{\bullet}$ at X-band frequencies; metalloradical or split signals, EPR signals in the $g = 2$ region attributed to the broadening of the Tyr Z$^{\bullet}$ spectrum by a weak spin−spin interaction with the Mn cluster; Q_A and Q_B, primary and secondary plastoquinone electron acceptors of PSII, respectively; Chl^+ and Car^+, chlorophyll and carotenoid cation radicals, respectively; MeOH, methanol; MES, 2-(*N*-morpholineethanesulfonic acid); chl, chlorophyll; duroquinone, tetramethyl-*p*-benzoquinone; NIR light, near-infrared light; EPR, electron paramagnetic resonance.

NO Treatment. NO at low concentrations eliminates the background spectrum of Tyr D$^{\bullet}$ (*40*−*42*) and also reduces rapidly the S_2 and S_3 states to S_1 (*43*) and more slowly S_1 to S_0 (*44*). It has been accordingly used to obtain samples without the background signal of Tyr D$^{\bullet}$ and also to enhance the S_0 population in samples that were advanced to S_0 by the administration of three light flashes (these samples would otherwise contain contributions from the other S states due to misses and double hits). NO was added only to samples poised in the S_0 state, and the treatment was carried out anaerobically at 0 °C inside the EPR tubes by slowly bubbling 4 mL of a 1:5 mixture of NO and N_2 for 1−2 min.

Illumination Conditions. Flash excitation of the samples was conducted with either of two studio photographic-flash power supplies: one with a nominal power of 600 W and a pulse duration of 2.1 ms, at temperatures below ca. 220 K, or one with a nominal power of 200 W and a pulse duration of 1.2 ms, used for single turnovers at −5 °C. To synchronize all PSII centers in the S_1 stable state, one preflash was given to the samples at −5 °C followed by a 30 min dark adaptation at 5 °C.

The S_2...Q_A(±MeOH) state was produced by single-flash illumination at −5 °C of the S_1 state, followed by a 30 s incubation at the same temperature, in the dark, to allow transfer of electrons from Q_A^- to duroquinone. This produced ∼80% of S_2 and no detectable amounts of S_3. S_2 was subsequently maximized by a strong flash at 190 K followed by transfer to −5 °C for 30 s (to activate transfer of an electron from Q_A^- to duroquinone). The S_0...Q_A(±MeOH) state was produced by administration of three flashes, spaced by 30 s, of samples that were previously poised in the S_1 state.

The $S_2Y_Z^{\bullet}$(+MeOH), $S_1Y_Z^{\bullet}$, and $S_0Y_Z^{\bullet}$(±MeOH) intermediates were produced by direct flash illumination (or in some cases by continuous illumination) inside the cavity at all temperatures that were examined. The $S_2Y_Z^{\bullet}$ intermediate was produced by direct flash illumination at >77 K. At lower temperatures, the S_2 configuration capable of producing the $S_2Y_Z^{\bullet}$ intermediate, S_2^t, was trapped by flash excitation of S_2 at 190 K followed by immediate transfer to liquid nitrogen, and from there into the EPR cryostat at 10 K (*28*). As S_2^t is stable over prolonged periods of time below 77 K, the $S_2Y_Z^{\bullet}$ intermediate was produced by flash illumination, inside the cavity, at each respective temperature below 77 K.

Elimination of Contributions from Other Species. Illumination at cryogenic temperatures produces, in addition to the Tyr Z$^{\bullet}$ radical, small amounts of the chl$^+$ and car$^+$ cation radicals. These are much less efficient electron donors than Tyr Z (*22*). The EPR signals of these species are narrow and can be easily discerned when present. These signals also saturate easily and decay much more slowly than the Tyr Z$^{\bullet}$ radical signal. The contribution of these minority species in the spectra was eliminated or suppressed by the use of flash illumination, high microwave power, and light−dark difference spectroscopy. Cyt b_{559} is also oxidized to a small extent, but its spectrum has no spectral overlap with the SnY_Z radicals. Besides, oxidized cyt b_{559} is very stable; therefore, it should not appear in the difference spectra.

Samples that advance to the S_0 state by our protocol (three flashes with NO treatment; see above) inevitably contain contributions from the S_1 state. The use of MeOH eliminates the S_1Y_Z EPR signal, which would otherwise interfere with the $S_0Y_Z^{\bullet}$ split signal.

EPR Measurements. EPR measurements were performed with an extensively upgraded former Bruker ER-200D spectrometer interfaced with a personal computer running appropriate software in the LabView programming environment. The Signal-Channel unit was replaced with an SR830 digital lock-in amplifier by Stanford Research. The spectrometer was equipped with an Oxford ESR 900 cryostat, an Anritsu MF76A frequency counter, and a Bruker 035M NMR gaussmeter. The perpendicular 4102ST cavity was used, the microwave frequency 9.408 GHz, the modulation frequency 100 kHz, and the modulation amplitude 8 Gpp (above 40 K) and 12.5 Gpp (below 40 K) in all experiments.

For the rapid-scan experiments, a multifunction NI 6251 pci card from National Instruments (16bit/1.25 MS/s) was used. Synchronization of the data acquisition with the magnetic field ramp produced by the Time Base unit was achieved by triggering the AD converter with a TTL pulse produced by the Time Base unit at the beginning of each scan. The spectra represent the average of the first 10 scans recorded 0.5 s after the flash minus the average of 10 or more spectra recorded after the signal had decayed. Construction of spectra was based on knowledge of the lifetimes of intermediates, and their temperature dependence; for instance, the decay rate of the $S_2Y_Z^{\bullet}$ intermediate, at 135 K, follows biphasic kinetics with a $t_{1/2}$(fast) of 3.8 s (40%) and a $t_{1/2}$(slow) of 55 s (60%) (manuscript in preparation).

RESULTS

In the study by Fielding et al. (*34*), the splitting of the nitroxide radical signal due to the spin−spin interaction with the iron(III) collapsed progressively as the temperature increased in the range of 8−120 K. Partial collapsing of the splitting was observed at ∼34 K, while the effect was completed above ∼60 K. A qualitatively similar behavior was observed by Szalai et al. in their study of the $S_2Y_Z^{\bullet}$ intermediate, trapped in inhibited PSII centers (*35*). We have examined the temperature dependence of five metalloradical intermediates, $S_0Y_Z^{\bullet}$(±5% MeOH), $S_1Y_Z^{\bullet}$, and $S_2Y_Z^{\bullet}$(±5% MeOH) of oxygen-evolving preparations.

Temperature Variation of the Tyr Z$^{\bullet}$-Based EPR Signals. Difference spectra in the range of 10−230 K for the intermediates are shown in Figure 1. The intermediate $S_0Y_Z^{\bullet}$(−MeOH) is not included since its spectrum contains potential contributions from the $S_1Y_Z^{\bullet}$ intermediate, and this would complicate the interpretation. Test runs in the temperature range of 7−35 K showed, however, behavior similar to that of the other intermediates. The spectra at the lowest-temperature end have been discussed in detail in earlier studies (*17*, *22*−*31*). Briefly, they consist of a characteristic split signal in addition to a less well-defined contribution at $g = 2.0$. The $g = 2.0$ region contains also potential contributions from side donors such as chl$^+$ or car$^+$; these are characterized by narrow radical spectra, which saturate easily. As these species are less efficient donors and decay considerably more slowly than Tyr Z$^{\bullet}$, their contribution to the spectra is minimized by the use of flash illumination, a high microwave power in recording the spectra, and light−dark difference spectroscopy (see Materials and Methods). The peak−trough separation varies among the different

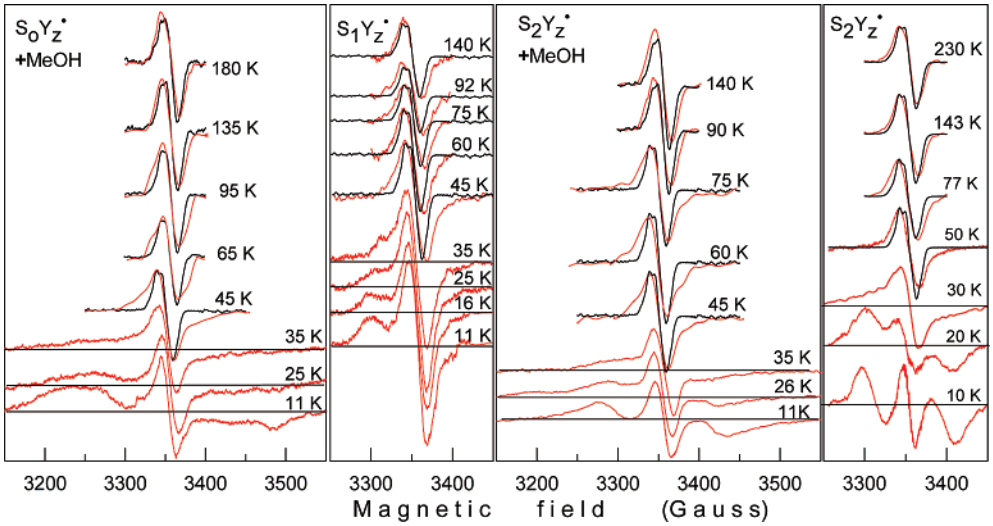

FIGURE 1: Temperature variation of the EPR spectra of four tyrosyl Z•-based intermediates (red traces). Spectra recorded below 40 K are regular scans (sweep time of 50 s and time constant of 30 ms) and represent the differences of the spectra recorded immediately after flash illumination minus the spectra recorded after the signal had decayed at each respective temperature. Those above 45 K are rapid scans (sweep time of 0.5 s and time constant of 3 ms for sweep fields of 200 G and sweep time of 0.2 s and time constant of 3 ms for sweep fields of 100 G) and represent the average of the first 10 spectra recorded 0.5 s after the flash minus the average of 10 or more spectra recorded after the signal had decayed. Spectra of the stable $Y_D^\bullet$ radical (black traces), recorded prior to flash illumination at each respective temperature under nonsaturating conditions. EPR settings: microwave frequency, 9.408 GHz; modulation frequency, 100 kHz; temperatures as indicated; microwave power, 100 mW (red traces) or 12.6 μW (black traces); modulation amplitude, 8 Gpp (>40 K) or 12.5 Gpp (<40 K) for both the $Y_Z^\bullet$ and $Y_D^\bullet$ spectra.

intermediates. It is smallest in the $S_2Y_Z^\bullet$ case (116 G), and it increases to 160 G in the presence of methanol and becomes ca. 240 G in the case of the $S_0Y_Z^\bullet$(+MeOH) signal. The latter is coincidentally comparable to the splitting of the $S_2Y_Z^\bullet$ signal in the case of the acetate-treated samples (*35*).

A progressive narrowing of the spectra is observed in Figure 1 as the temperature is increased above 20 K. At 45 K, the magnetic splitting is reduced considerably, and above ~100−120 K, it collapses completely to a radical spectrum. This effect can be more easily discerned by examination of the spectra normalized with respect to temperature (intensity multiplied by temperature), and even more notably by examination of the integrated spectra, as suggested by Fielding et al. (*34*). Panels A and B of Figure 2 present such plots for the case of the $S_0Y_Z^\bullet$ signal obtained in samples containing methanol. Qualitatively similar behavior is observed with the other signals as well.

We have conducted a calculation similar to that described by Szalai et al. (*35*; see also ref *45*) using the published T_1 values for the S_2 multiline in untreated (*46*) or methanol-treated samples (*47*) or the S_0(+MeOH) multiline (*48*). The calculation has yielded values of 25−28 K for the temperature at which averaging of the magnetic interaction of Tyr Z• with the Mn cluster should begin to occur in the three cases. These values are compatible with the spectra of Figure 1 within theoretical and experimental error.

Microwave Power Dependence. A common property of all spectra in Figure 1 is the lack of significant saturation at the highest power. No power dependence could be detected above 77 K at three different microwave powers, 100, 25, and 6.3 mW.

Examination of the High-Temperature Spectra. The experiments described above suggest that the split signal at liquid-helium temperatures progressively collapses to the narrow signal at elevated temperatures. The collapsing is

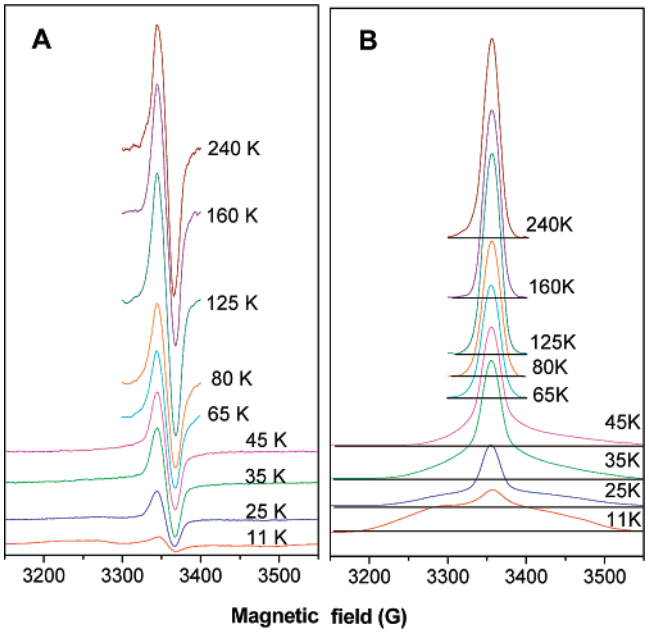

FIGURE 2: Temperature variation of the normalized $S_0Y_Z^\bullet$(+MeOH) spectra (different set of spectra from those of Figure 1) (A) after multiplication of the intensities with the respective temperature value and (B) integration of the spectra in panel A. EPR conditions as in Figure 1.

practically complete above ~100−120 K in all cases. Figure 3 compares the $S_2Y_Z^\bullet$ spectra at 140 K (blue trace) and 190 K (red trace). The traces are practically superimposable with a slight deviation in the middle, which is due to a minor impurity of a narrow radical contribution in the spectrum at 190 K. The two $S_2Y_Z^\bullet$ spectra are also compared with the spectrum of Tyr D• recorded at the same microwave power (black trace), at 100 mW (saturation very pronounced at this microwave power), or under nonsaturating conditions (green trace). Clearly, the $S_2Y_Z^\bullet$ signal is significantly broader, ~25 G wide, than the spectrum of Tyr D•, ~18 G wide. Identical,

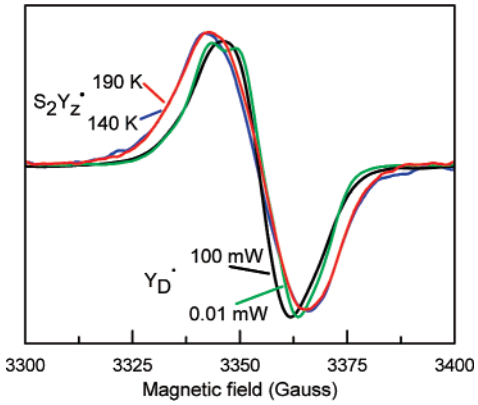

FIGURE 3: Superposition of the $S_2Y_Z^\bullet$ spectra at 140 K (blue trace) and 190 K (red trace) and comparison with the spectrum of Tyr D$^\bullet$. The latter was recorded at 140 K under saturating (100 mW, black trace) or nonsaturating (0.01 mW, green trace) conditions. The spectra are rapid scans (sweep time of 0.2 s and time constant of 3 ms), recorded with a power of 100 mW (except for the green trace) and a modulation amplitude of 8 Gpp. The spectra have been arbitrarily normalized.

within signal to noise, Tyr Z$^\bullet$ spectra were recorded in the other S states and in the presence or absence of methanol (not shown).

DISCUSSION

These results demonstrate a progressive narrowing of the split spectra of all intermediates with increasing temperatures (Figures 1 and 2), consistent with the increase in the Mn spin−lattice relaxation rate. This results in the averaging of the spin−spin coupling between $Y_Z^\bullet$ and the Mn cluster, and the appearance of the unperturbed $Y_Z^\bullet$ spectrum, a narrow signal ~25 G wide, at elevated temperatures (Figure 3). One may note the absence of hyperfine features in the spectra of Figure 3. This is due to the high modulation amplitude (8 Gpp) used in these studies for the purpose of enhancing the signal to noise ratio. In a manuscript being prepared for publication, we present and analyze higher-resolution spectra obtained with 4 or 2 G modulation. These exhibit well-resolved hyperfine features. At the current resolution, no differences are observed in the elevated-temperature $Y_Z^\bullet$ spectra among the different intermediates. This strengthens the assignment of all intermediates to $Y_Z^\bullet$, and it also suggests that no major changes occur in the tyrosine in the different S states (S_0, S_1, or S_2) or in the presence of methanol. Fine differences may, however, be present at higher resolution and particularly after the potential future employment of high-frequency high-field EPR spectroscopy. Certain limitations on the quantitative evaluation of the spectra in Figures 1 and 2 are discussed below. Comments on the reliability of the signal shape production and rather overwhelming arguments in favor of the assignment of the 25 G signal to $Y_Z^\bullet$ and some additional comments are presented subsequently.

Limitations on Spin Quantitation. In the case of the $S_0Y_Z^\bullet$ and $S_2Y_Z^\bullet$ intermediates, the ground state of the Mn cluster is an isolated $S = {}^1/_2$ doublet (*46*−*48*); therefore, the split Tyr Z$^\bullet$ signal at 11 K should represent all centers where Tyr Z was oxidized. The case of $S_1Y_Z^\bullet$ is less clear, because the ground state is not an isolated doublet (*49*, *50*) and appropriate Boltzman factors and transition probabilities should be taken into account for spin quantitation at liquid-helium temperatures (*26*). The $S_1Y_Z^\bullet$ signal is also very unstable above 77 K because the S_1 to S_2 transition is the only transition which is activated above ~77 K (ref *17* and our unpublished results). Another factor that limits the quantitative comparison of the spectra at different temperatures is the following. Unlike the case of the $S_2Y_Z^\bullet$ signal in inhibited samples (*35*), which is indefinitely stable at cryogenic temperatures, the metalloradical signals in the intact system decay quickly and need to be reinduced at each respective temperature. As the efficiency of the signal induction is not necessarily constant throughout the entire temperature range, this creates an uncertainty, which is somewhat reduced by the following consideration. At very low temperatures, the efficiency of the signal production should be smaller, while the faster decay of the signal at higher temperatures could result in the trapping of smaller fractions.

Advantages Set by the Fast Decay of the Signals. The fast decay of the signals and the need to reinduce them at each respective temperature have, however, important advantages. Both the light-induced Tyr Z$^\bullet$ signal and the background spectrum obtained after decay of the Tyr Z$^\bullet$ signal are recorded at exactly the same temperature, resulting in very reliable light−dark signal shapes. This is critical especially at elevated temperatures where the strong background radical signals could interfere strongly with the light-induced one. Most importantly, production of side donors is minimized due to the low temperature of illumination and can be easily corrected on the basis of their different decay times (see Materials and Methods). In contrast, production of Tyr Z$^\bullet$ in inhibited samples requires illumination at temperatures close to 0 °C or higher. This produces significant amounts of Tyr D$^\bullet$, which, as noted recently, are difficult to separate from the Tyr Z$^\bullet$ spectrum (*36*).

The Intensity of the High-Temperature Signal Is S-State-Dependent and Therefore Associated with Active Centers. The intensity of the light-induced transient signal at elevated temperatures is S-state-dependent: The transient $S_1Y_Z^\bullet$ signals detected above ~140 K are much smaller than in the case of the S_0 and S_2 states, and practically no transient can be detected at ≥180 K. This is compatible with the fact that S_1 advances to S_2 with increasing efficiency as the temperature is increased above ~80−100 K (ref *17* and our unpublished results), while all other S-state transitions require temperatures higher than 230 K (*51*). This rules out the unlikely possibility that the high-temperature transient is due to a minority of inactive centers (actually no transient Tyr Z signals can be induced at cryogenic temperatures in any of the inhibited or inactive PSII preparations).

Excluding Alternative Origins of the High-Temperature Spectra. The high-temperature spectra cannot be due to relaxation enhancement of Tyr D$^\bullet$ (*52*), because they are broader than signal II. Also in samples poised in the S_0(+MeOH) state the Tyr D$^\bullet$ signal intensity was negligible due to the NO treatment (see Materials and Methods), yet the intensity of the light-induced "25 G signal" was significant. Furthermore, the low- and high-temperature signals are not saturated at the highest microwave power. This behavior discriminates them from isolated radicals like Tyr D$^\bullet$, carotenoid, and chlorophyll, which, as expected, are saturated at low microwave powers. The lack of saturation

does not, however, exclude a contribution from Q_A^- at elevated temperatures. Q_A acts as the electron acceptor during the charge separation at cryogenic temperatures, and the magnetic interaction with the non-heme iron strongly enhances the relaxation rate of Q_A^-. It can be argued that the magnetic splitting of Q_A^- is much too large for this kind of exchange narrowing to take place. However, to test whether Q_A^- is observable at elevated temperatures, we conducted the following simple experiment. Samples in the S_1 state were illuminated continuously for 4 min at 200 K to produce $S_2...Q_A^-$. The $g = 2$ region of the spectra was recorded before and after the illumination under a low microwave power. The spectrum before illumination was that of Tyr $D^\bullet$ representing by a rough estimation 70% of centers. No evidence for an increase in the signal intensity was present, except for minor contributions from chlorophyll or carotenoid radicals, although the concentration of Q_A^- produced by this experiment was comparable or higher than the initial concentration of $Y_D^\bullet$.

Linking the Low-Temperature Photochemistry to the High-Temperature Photochemistry. The split $S_1Y_Z^\bullet$ signal (11 K) is a true intermediate of the S_1 to S_2 transition, as it advances to S_2 when heated rapidly to 200 K (*17*, *31*). An important observation linking the elevated to the low-temperature photochemistry is the following. Flash illumination in the range of 77−190 K of samples prepared in the $S_2...Q_A$ state produces a transient state, which according to these experiments is characterized by the 25 G signal. It has been observed earlier that this transient state advances to S_3 at −10 °C while on rapid cooling to 10 K gives rise to the $S_2Y_Z^\bullet$ metalloradical EPR signal (*28*). These observations are entirely consistent with the assignment of the 25 G radical to Tyr $Z^\bullet$, the natural intermediate of the S-state transitions. Accordingly, the liquid-helium- and elevated-temperature spectra are manifestations of the same intermediate, except that the EPR spectra at 11 K are perturbed by the magnetic interaction of Tyr $Z^\bullet$ with the Mn cluster.

The observations in this paper provide a convenient way to probe by EPR spectroscopy the long-sought Tyr $Z^\bullet$ intermediate undisturbed by the magnetic interaction with the Mn cluster. These observations open up the way to the detailed characterization of Tyr $Z^\bullet$ in various S states and potentially during S-state turnover.

ACKNOWLEDGMENT

We thank Dr. Y. Sanakis for helpful discussions.

REFERENCES

1. Goussias, C., Boussac, A., and Rutherford, A. W. (2002) Photosystem II and photosynthetic oxidation of water: An overview, *Philos. Trans. R. Soc. London, Ser. B 357*, 1369−1381.
2. Carrell, T. G., Tyryskin, A. M., and Dismukes, G. C. (2002) An evaluation of structural models for the photosynthetic water-oxidizing complex derived from spectroscopic and X-ray diffraction signatures, *J. Biol. Inorg. Chem. 7*, 2−22.
3. Britt, R. D., Campbell, K. A., Peloquin, J. M., Gilchrist, M. L., Aznar, C. P., Dicus, M. M., Robblee, J., and Messinger, J. (2004) Recent pulsed EPR studies of the Photosystem II oxygen-evolving complex: Implications as to water oxidation mechanisms, *Biochim. Biophys. Acta 1655*, 158−171.
4. Yachandra, V. K. (2005) The Catalytic Manganese Cluster: Organization of the Metal Ions, in *Photosystem II: The Water/Plastoquinone Oxido-Reductase of Photosynthesis* (Wydrzynski, T., and Satoh, K., Eds.) pp 235−260, Kluwer Academic Publishers, Dordrecht, The Netherlands.
5. Hillier, W., and Messinger, J. (2005) Mechanism of Photosynthetic Oxygen Production, in *Photosystem II: The Water/Plastoquinone Oxido-Reductase of Photosynthesis* (Wydrzynski, T., and Satoh, K., Eds.) pp 567−608, Kluwer Academic Publishers, Dordrecht, The Netherlands.
6. Haumann, M., Liebisch, P., Müller, C., Barra, M., Grabolle, M., and Dau, H. (2005) Photosynthetic O_2 formation tracked by time-resolved X-ray experiments, *Science 310*, 1019−1021.
7. McEvoy, J. P., and Brudvig, G. W. (2006) Water-Splitting Chemistry of Photosystem II, *Chem. Rev. 106*, 4455−4483.
8. Zouni, A., Witt, H. T., Kern, J., Fromme, P., Krauss, N., Saenger, W., and Orth, P. (2001) Crystal structure of photosystem II from *Synechococcus elongatus* at 3.8 Å resolution, *Nature 409*, 739−743.
9. Kamiya, N., and Shen, J. R. (2003) Crystal structure of oxygen-evolving photosystem II from *Thermosynechococcus vulcanus* at 3.7-Å resolution, *Proc. Natl. Acad. Sci. U.S.A. 100*, 98−103.
10. Ferreira, K. N., Iverson, T. M., Maghlaoui, K., Barber, J., and Iwata, S. (2004) Architecture of the photosynthetic oxygen-evolving center, *Science 303*, 1831−1838.
11. Loll, B., Kern, J., Saenger, W., Zouni, A., and Biesiadka, J. (2005) Towards complete cofactor arrangement in the 3.0 Å resolution structure of photosystem II, *Nature 438*, 1040−1044.
12. Yano, J., Kern, Y., Sauer, K., Latimer, M. J., Pushkar, Y., Biesiadka, J., Loll, B., Saenger, W., Messinger, J., Zouni, A., and Yachandra, V. (2006) Where water is oxidized to dioxygen: Structure of the photosynthetic Mn_4Ca cluster, *Science 314*, 821−825.
13. Pushkar, Y., Yano, J., Glatzel, P., Messinger, J., Lewis, A., Sauer, K., Bergmann, U., and Yachandra, V. (2007) Structure and Orientation of the Mn_4Ca Cluster in Plant Photosystem II Membranes Studied by Polarized Range-extended X-ray Absorption Spectroscopy, *J. Biol. Chem. 282*, 7198−7208.
14. Diner, B. A., and Britt, R. D. (2005), The redox-active tyrosines Y_Z and Y_D, in *Photosystem II: The Light-Driven Water:Plastoquinone Oxidoreductase* (Wydrzynski, T. J., and Satoh, K., Eds.) pp 207−233, Advances in Photosynthesis and Respiration 22, Springer, Dordrecht, The Netherlands.
15. Meyer, T. J., Huynh, M. H. V., and Thorp, H. H. (2007) The Possible Role of Proton-Coupled Electron Transfer (PCET) in Water Oxidation by Photosystem II, *Angew. Chem., Int. Ed. 46*, 5284−5304.
16. Hoganson, C. W., and Babcock, G. T. (1988) Electron-transfer events near the reaction center in O_2-evolving photosystem II preparations, *Biochemistry 27*, 5848−5855.
17. Nugent, J. H. A., Muhiuddin, I. P., and Evans, M. C. W. (2002) Electron transfer from the water oxidizing complex at cryogenic temperatures: The S_1 to S_2 step, *Biochemistry 41*, 4117−4126.
18. Nugent, J. H. A., Turconi, S., and Evans, M. C. W. (1997) EPR Investigation of Water Oxidizing Photosystem II: Detection of New EPR Signals at Cryogenic Temperatures, *Biochemistry 36*, 7086−7096.
19. Ioannidis, N., and Petrouleas, V. (2000) Electron paramagnetic resonance signals from the S_3 state of the oxygen-evolving complex. A broadened radical signal induced by low-temperature near-infrared light illumination, *Biochemistry 39*, 5246−5254.
20. Ioannidis, N., Nugent, J. H. A., and Petrouleas, V. (2002) Intermediates of the S_3 State of the Oxygen-Evolving Complex of Photosystem II, *Biochemistry 41*, 9589−9600.
21. Geijer, P., Morvaridi, F., and Styring, S. (2001) The S_3-state of the oxygen-evolving complex in photosystem II is converted to the $S_2Y_Z^\bullet$ at alkaline pH, *Biochemistry 40*, 10881−10891.
22. Zhang, C. X., and Styring, S. (2003) Formation of split electron paramagnetic resonance signals in photosystem II suggests that tyrosine Z can be photooxidized at 5 K in the S_0 and S_1 states of the oxygen-evolving complex, *Biochemistry 42*, 8066−8076.
23. Koulougliotis, D., Shen, J. R., Ioannidis, N., and Petrouleas, V. (2003) Near-IR irradiation of the S_2 state of the water oxidizing complex of photosystem II at liquid helium temperatures produces the metalloradical intermediate attributed to $S_1Y_Z^\bullet$, *Biochemistry 42*, 3045−3053.
24. Nugent, J. H. A., Muhiuddin, I. P., and Evans, M. C. W. (2003) Effects of Hydroxylamine on Photosystem II: Reinvestigation of Electron Paramagnetic Resonance Characteristics Reveals Possible S State Intermediates, *Biochemistry 42*, 5500−5507.
25. Zhang, C. X., Boussac, A., and Rutherford, A. W. (2004) Low-Temperature Electron Transfer in Photosystem II: A Tyrosyl Radical and Semiquinone Charge Pair, *Biochemistry 43*, 13787−13795.

26. Koulougliotis, D., Teutloff, C., Sanakis, Y., Lubitz, W., and Petrouleas, V. (2004) The $S_1Y_Z^{\bullet}$ metalloradical intermediate in Photosystem II: An X- and W-band EPR study, *Phys. Chem. Chem. Phys. 6*, 4859−4863.
27. Petrouleas, V., Koulougliotis, D., and Ioannidis, N. (2005) Trapping of Metalloradical Intermediates of the S-States at Liquid Helium Temperatures. Overview of the Phenomenology and Mechanistic Implications, *Biochemistry 44*, 6723−6728.
28. Ioannidis, N., Zahariou, G., and Petrouleas, V. (2006) Trapping of the S2 to S3 state intermediate of the oxygen-evolving complex of photosystem II, *Biochemistry 45*, 6252−6259.
29. Havelius, K. G. W., Su, J. H., Feyziyev, Y., Mamedov, F., and Styring, S. (2006) Spectral resolution of the split EPR signals induced by illumination at 5 K from the S_1, S_3, and S_0 states in Photosystem II, *Biochemistry 45*, 9279−9290.
30. Su, J.-H., Havelius, K. G. V., Mamedov, F., Ho, F. M., and Styring, S. (2006) Split EPR Signals from Photosystem II Are Modified by Methanol, Reflecting S State-Dependent Binding and Alterations in the Magnetic Coupling in the $CaMn_4$ Cluster, *Biochemistry 45*, 7617−7627.
31. Sioros, G., Koulougliotis, D., Karapanagos, G., and Petrouleas, V. (2007) The $S_1Y_Z^{\bullet}$ Metalloradical EPR Signal of Photosystem II Contains Two Distinct Components That Advance Respectively to the Multiline and $g = 4.1$ Conformations of S_2, *Biochemistry 46*, 210−217.
32. Boussac, A., Sugiura, M., Lai, T.-L., and Rutherford, A. W. (2007) Low temperature photochemistry in Photosystem II from *Thermosynechococcus elongatus* induced by visible and near-infrared light. *Philos. Trans. R. Soc. London, Ser. B* (in press).
33. Su, J.-H., Havelius, K. G. V., Ho, F. M., Han, G., Mamedov, F., and Styring, S. (2007) Formation Spectra of the EPR Split Signals from the S0, S1, and S3 States in Photosystem II Induced by Monochromatic Light at 5 K, *Biochemistry 46*, 10703−10712.
34. Fielding, L., More, K. M., Eaton, G. R., and Eaton, S. S. (1986) Metal-Nitroxyl Interactions. 51. Collapse of Iron-Nitroxyl Electron-Electron Spin-Spin Splitting due to the Increase in the Electron Spin relaxation Rate for High-Spin Iron(III) when Temperature Is Increased, *J. Am. Chem. Soc. 108*, 8194−8196.
35. Szalai, V., Kühne, H., Lakshmi, K. V., and Brudvig, G. W. (1998) Characterization of the Interaction between Manganese and Tyrosine Z in Acetate-Inhibited Photosystem II, *Biochemistry 37*, 13594−13603.
36. Un, S., and Boussac, A., and Sugiura, M. (2007) Characterization of the Tyrosine-Z radical and Its Environment in the Spin-Coupled $S_2TyrZ^{\bullet}$ State of Photosystem II from *Thermosynechococcus elongatus*, *Biochemistry 46*, 3138−3150.
37. Berthold, D. A., Babcock, G. T., and Yocum, C. F. (1981) A Highly Resolved, Oxygen-Evolving Photosystem-II Preparation From Spinach Thylakoid Membranes: Electron-Paramagnetic-Resonance and Electron-Transport Properties, *FEBS Lett. 134*, 231−234.
38. Ford, R. C., and Evans, M. C. W. (1983) Isolation of a Photosystem-2 Preparation From Higher-Plants With Highly Enriched Oxygen Evolution Activity, *FEBS Lett. 160*, 159−164.
39. Petrouleas, V., and Diner, B. A. (1987) Light-induced oxidation of the acceptor-side Fe(II) of Photosystem II by exogenous quinones acting through the Q_B binding site. I. Quinones, kinetics and pH dependence, *Biochim. Biophys. Acta 893*, 126−137.
40. Petrouleas, V. V., and Diner, B. A. (1990) Formation by NO of Nitrosyl Adducts of Redox Components of the Photosystem II Reaction Center. I. NO Binds to the Acceptor-Side Non-Heme Iron, *Biochim. Biophys. Acta 1015*, 131−140.
41. Szalai, V. A., and Brudvig, G. W. (1996) Reversible binding of nitric oxide to tyrosyl radicals in photosystem II. Nitric oxide quenches formation of the S_3 EPR signal species in acetate-inhibited photosystem II, *Biochemistry 35*, 15080−15087.
42. Sanakis, Y., Goussias, Ch., Mason, R. P., and Petrouleas, V. (1997) NO interacts with the tyrosine radical $Y_D^{\bullet}$ of Photosystem II to form an iminoxyl radical, *Biochemistry 36*, 1411−1417.
43. Ioannidis, N., Schansker, G., Barynin, V. V., and Petrouleas, V. (2000) Interaction of nitric oxide with the oxygen evolving complex of Photosystem II and Mn-catalase. A comparative study, *J. Biol. Inorg. Chem. 5*, 354−363.
44. Ioannidis, N., Sarrou, J., Schansker, G., and Petrouleas, V. (1998) NO Reversibly Reduces the Water-Oxidizing Complex of Photosystem II through S_0 and S_{-1} to the State Characterized by the Mn(II)-Mn(III) Multiline EPR Signal, *Biochemistry 37*, 16445−16451.
45. Weil, J. A., Bolton, J. R., and Wertz, J. E. (1994) *Electron Paramagnetic Resonance Elementary Theory and Practical Applications*, John Wiley & Sons, Inc., New York.
46. Lorigan, G. A., and Britt, R. D. (1994) Temperature-Dependent Pulsed Electron Paramagnetic Resonance Studies of the S_2 state Multiline Signal of Photosynthetic Oxygen-Evolving Complex, *Biochemistry 33*, 12072−12076.
47. Peterson, S., Årling, K. A., and Styring, S. (1999) The EPR signals from the S_0 and S_2 states of the Mn Cluster in Photosystem II Relax Differently, *Biochemistry 38*, 15223−15230.
48. Kulik, L. V., Lubitz, W., and Messinger, J. (2005) Electron Spin-Lattice Relaxation of the Oxygen-Evolving Complex in Photosystem II and of Dinuclear Manganese Model Complexes, *Biochemistry 44*, 9368−9374.
49. Dexheimer, S. L., and Klein, M. P. (1992) Detection of a paramagnetic intermediate in the S_1 state of the photosynthetic oxygen-evolving complex, *J. Am. Chem. Soc. 114*, 2821−2826.
50. Yamauchi, T., Mino, H., Matsukawa, T., Kawamori, A., and Ono, T. (1997) Parallel polarization electron paramagnetic resonance studies of the S_1-state manganese cluster in the photosynthetic oxygen-evolving system, *Biochemistry 36*, 7520−7526.
51. Styring, S., and Rutherford, A. W. (1988) Deactivation kinetics and temperature dependence of the S-state transitions in the oxygen-evolving system of Photosystem II measured by EPR spectroscopy, *Biochim. Biophys. Acta 933*, 378−387.
52. Boussac, A., and Rutherford, A. W. (1995) Does the Formation of the S_3-State in Ca^{2+}-Depleted Photosystem-II Correspond to an Oxidation of Tyrosine-Z Detectable by Cw-Epr at Room-Temperature, *Biochim. Biophys. Acta 1230*, 195−201.

BI7018767